Journal Pre-proof

Targeting Fungal Virulence Factor by Small Molecules: Structure-based Discovery of Novel Secreted Aspartic Protease 2 (SAP2) Inhibitors

Chenglan Li, Yang Liu, Shancao Wu, Guiyan Han, Jie Tu, Guoqiang Dong, Na Liu, Chunquan Sheng

PII: S0223-5234(20)30487-6

DOI: https://doi.org/10.1016/j.ejmech.2020.112515

Reference: EJMECH 112515

To appear in: *European Journal of Medicinal Chemistry*

Received Date: 22 March 2020

Revised Date: 19 May 2020

Accepted Date: 29 May 2020

Please cite this article as: C. Li, Y. Liu, S. Wu, G. Han, J. Tu, G. Dong, N. Liu, C. Sheng, Targeting Fungal Virulence Factor by Small Molecules: Structure-based Discovery of Novel Secreted Aspartic Protease 2 (SAP2) Inhibitors, *European Journal of Medicinal Chemistry*, https://doi.org/10.1016/j.ejmech.2020.112515.

Graphical Abstract

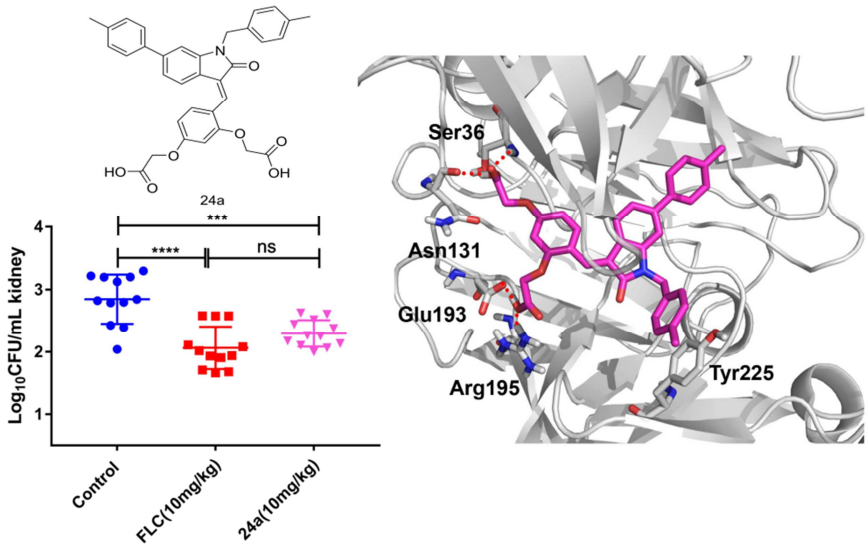

Targeting Fungal Virulence Factor by Small Molecules: Structure-based Discovery of Novel Secreted Aspartic Protease 2 (SAP2) Inhibitors

Chenglan Li [a, b, 1], Yang Liu [c, 1], Shancao Wu [b, 1], Guiyan Han [b], Jie Tu [b], Guoqiang Dong [b, *], Na Liu [b, *], Chunquan Sheng [a, b, *]

a. School of Pharmacy, Ningxia Medical University, 1160 Shengli Street, Yinchuan 750004, China

b. Department of Medicinal Chemistry, School of Pharmacy, Second Military Medical University, 325 Guohe Road, Shanghai 200433, China

c. Department of Pharmacy, No. 971 Hospital of PLA, Qingdao 266071, China

* Corresponding authors

E-mail address: shengcq@smmu.edu.cn (C. Sheng), liuna66@aliyun.com (N. Liu), dgq-81@163.com (G. Dong)

[1] These authors contributed equally to this work

Abstract

Secreted aspartic protease 2 (SAP2), a kind of virulence factor, is an emerging new antifungal target. Using docking-based virtual screening and structure-based inhibitor design, a series of novel SAP2 inhibitors were successfully identified. Among them, indolone derivative **24a** showed potent SAP2 inhibitory activity (IC_{50} = 0.92 μM). It blocked fungi biofilm and hypha formation by down-regulating the expression of genes *SAP2*, *ECE1*, *ALS3* and *EFG1*. As a virulence factor inhibitor, compound **24a** was inactive in vitro and showed potent in vivo efficacy in a murine model of invasive candidiasis. It represents a promising lead compound for the discovery of novel antifungal agents.

KEY WORDS: Secreted aspartic protease 2, antifungal, virulence factor.

1. Introduction

Invasive Candida infections increase dramatically in recent years, representing a serious disease with high morbidity and mortality [1]. Antifungal agents including azoles, polyenes and chinocandins are used as frontline treatments of invasive candidiasis. However, pathogenic fungi can be only controlled ephemerally due to the rapid development of resistance [2-4]. Thus, discovery of novel antifungal agents acting on new targets is urgently needed. Secreted aspartic proteases (SAPs) were proven to be a crucial virulent factor during fungal infections [5, 6] . There are 10 SAP genes (SAP1-10) in the *C. albicans* genome [5, 7]. SAP genes in *Candida parapsilosis* (*C. parapsilosis*), *Candida tropicalis* (*C. tropicalis*) and *Candida dubliniensis* (*C. dubliniensis*) are orthologous genes [8-11]. SAP1-3 are secreted mainly in yeast form of *C. albicans*, while SAP4-6 are secreted in hypha form [12, 13]. Among them, the structure and function of SAP2 has been extensively studied, which was supposed to be a potential target for the development of novel antifungal agents.

Fungi biofilms (particularly *Candida*) are often highly assembled on the surface of medical devices implanted in individual patients and epithelial cells, which cause the development of drug resistance [14-17]. SAPs were regarded as important factors for biofilm formation [13, 18]. It is reported that SAPs production enhanced the exposure of *C. albicans* biofilms to sub-inhibitory concentrations of fluconazole (FLC) [13, 18]. However, the effects of SAP2 inhibitors on the biofilm formation still remain unknown.

Peptide and peptidominetic SAP2 inhibitors have been reported [19]. However, most of them lack antifungal potency possibly due to unfavorable physicochemical and pharmacokinetic properties. Thus, the identification of small molecule SAP2 inhibitors is highly desirable for target validation and antifungal lead discovery. In our previous studies, the first class of SAP2 inhibitors were identified by virtual screening of the SPECS database [19]. Inspired by this proof-of-concept study, there is an urgent

need to design structurally diverse SAP2 inhibitors, which can be used as chemical probes or lead compounds to explore biological and pharmacological functions of SAP2 and discover novel antifungal agents.

To design new classes of SAP2 inhibitors, herein structure-based virtual screening was performed using a larger compound library. After structure-based hit optimization, a series of new SAP2 inhibitors were discovered. Among them, indolone inhibitor 24a showed potent SAP2 inhibitory activity and could significantly reduce the kidney fungal burdens in a murine model of invasive candidiasis. Importantly, the biofilm inhibitory activity of SAP2 inhibitors was confirmed for the first time. Compound 24a significantly inhibited biofilm formation and filamentation of azole-resistant *C. albicans* and *C. tropicalis*.

2. Results and Discussion

2.1 Structure-based Virtual Screening of the ChemDiv Database

The virtual screening procedure is similar to that of our previous protocol (**Fig. 1A**) [19]. A total of about 713,000 compounds in ChemDiv database were docked and ranked by GOLD, which was proven to be an accurate method to dock SAP2 inhibitors. The fitness score of 85 was used as a cutoff value for the selection of the initial hits. As a result, top-ranked 7851 molecules were obtained and subjected to docking validation and visual inspection. The selection of the candidate molecules was based the following criteria: (1) effective mimicking of the interaction of peptide inhibitor A70450; (2) formation of hydrogen bonding interactions with residues involved in A704500-SAP2 interaction; (3) compounds with too many rotatable bonds were excluded for further evaluation; (4) the binding mode of the compounds can be reproduced by at least two docking methods. After filtration, 582 candidate compounds were subjected to similarity analysis and 100 structurally diverse candidates were designated for purchase. Finally, only 50 compounds turned out to be commercially available for in vitro assaying (**Fig. S1** in Supporting Information).

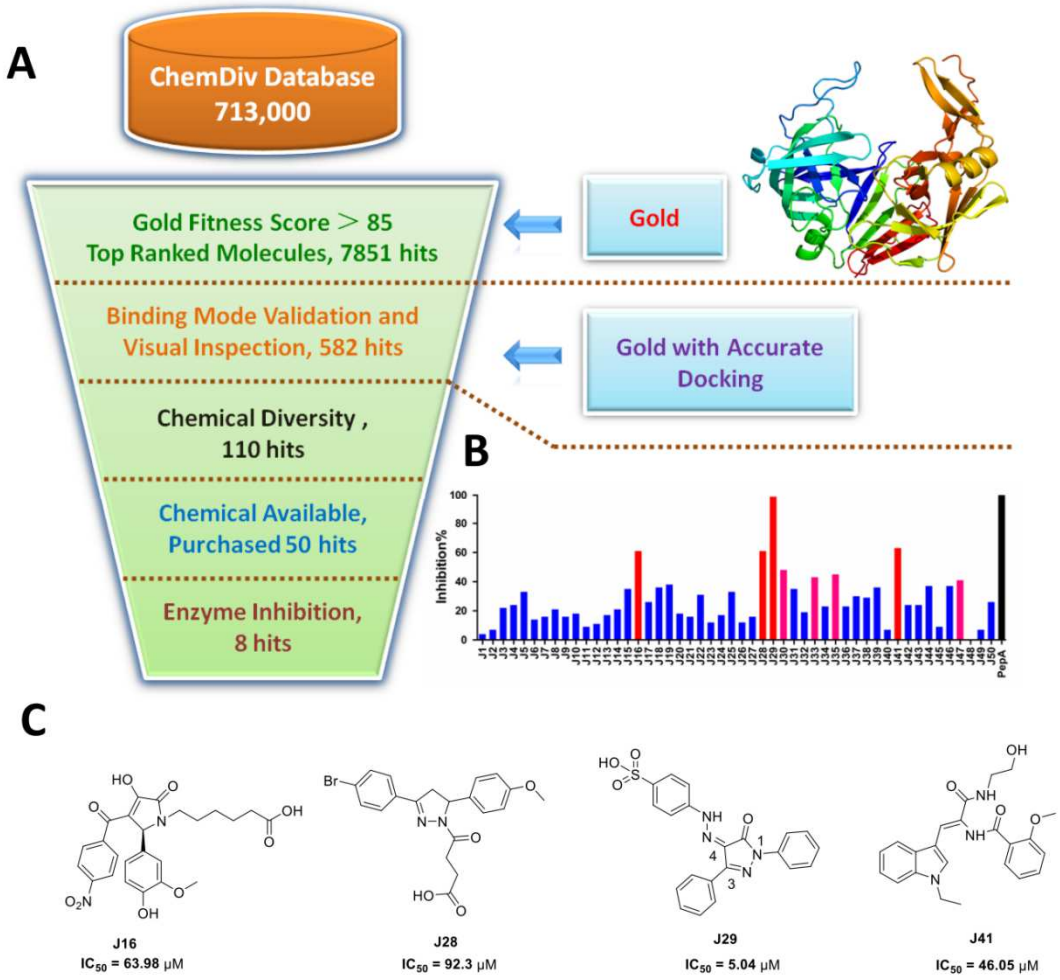

Fig. 1 Discovery of new SAP2 inhibitors by virtual screening. (A) Protocol for virtual screening of small-molecule SAP2 inhibitors; (B) SAP2 inhibitory activity of compounds selected from virtual screening at the concentration of 100 μM. (C) Chemical structures and inhibitory activity of four novel SAP2 inhibitors.

2.2 SAP2 Inhibitory Activity Assay and Molecular Docking

Using a spectrophotometric assay [20-23], initial screening of *C. albicans* SAP2 inhibitory activity was performed at the concentration of 100 μM. Peptide inhibitor pepstatin A (PepA) was used as the positive control. The results revealed that 8 out of 50 compounds showed an inhibitory rate larger than 40% with a hit rate of 16% (**Fig. 1B** and **Table S1** in Supporting Information). The IC_{50} values were further determined for 4 compounds with inhibitory rate larger than 50% and their IC_{50} values are in the

range of 5.04 μM to 92.3μM (**Fig. 1C**). Among them, compound **J29** showed the best SAP2 inhibitory activity (IC_{50} = 5.04 μM). Then, the binding mode of inhibitor **J29** was investigated by molecule docking. As shown in **Fig. 2**, it bound with SAP2 by mimicking the interaction of A704500. The pyrazolone scaffold was located at the central site of S1, S2, S1' and S2' pocket. The C1, C3 and C4 side chain of pyrazolone interacted with the S1', S1 and S2 pocket, respectively. The C3-phenyl group formed aromatic π-π interaction with Tyr84 and hydrophobic interactions with Ile30, Ile119 and Ile123. The C4 phenyl group formed hydrophobic interactions with Ile 305 and Ile223. Notably, the terminal sulfonic acid group of the C4-side chain formed two hydrogen bonds with Tyr225.

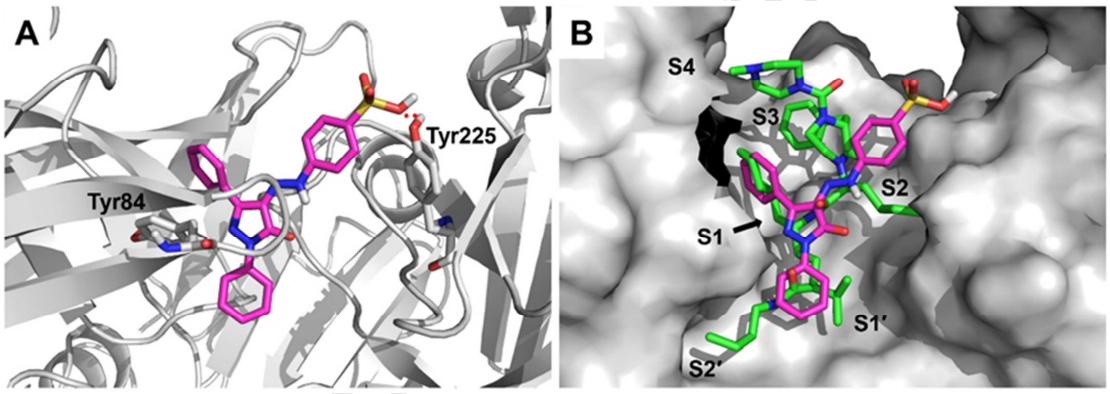

Fig. 2 Binding modes of pyrazolone SAP2 inhibitor **J29**. (A) Proposed binding pose of inhibitor **J29** in the active site of SAP2. The inhibitors are shown in the stick format and hydrogen bonds are shown in dotted red lines. (B) The comparison of binding modes of small-molecule inhibitor **J29** (carbon atoms in purple) with peptide inhibitor A-70450 (carbon atoms in green) are shown on the surface of SAP2. The ligand binding pockets of SAP2 are labeled on the surface of the active site. The figures are generated using PyMol (http://www.pymol.org).

*2.3 Structure-Activity Relationship (SAR) of Pyrazolone SAP2 Inhibitor **J29***

Compound J29 was reported as a Shp-2 inhibitors for the treatment of cancer and the benzenesulfonic acid group is necessary for the activity [24]. To validate the importance of sulfonic acid in hydrogen bonding interaction with SAP2, compounds without C-ring acid group were designed and synthesized (**6a-6e**). Moreover, the

diazanyl group was unfavorable for the drug-like properties, which was removed in the following SAR studies (**Fig. 3**). In consistence with the binding mode, these compounds were almost inactive at the concentration of 100 μM (**Table 1**). Then, a series of compounds with C-ring acid bioisosteres were synthesized and assayed (**5a-5y**). The SAP2 inhibitory activity was retained for most of the target compounds, further highlighting the importance of the acid group. For the carboxylic derivatives, compounds with di-carboxylic side chains were generally more active than the mono-substituted analogues. Moreover, the 2,4-disubstitution was better than the 3,4-disubstitution. Compounds **5m** (IC_{50} = 10.05 μM) and **5o** (IC_{50} = 10.75 μM) are best compounds in this series. Moreover, A-ring substitutions also had different effects on the SAP2 inhibitory activity. Among the di-substituted derivatives, the 4-chloro substitution or no substitution were generally more favorable for the activity.

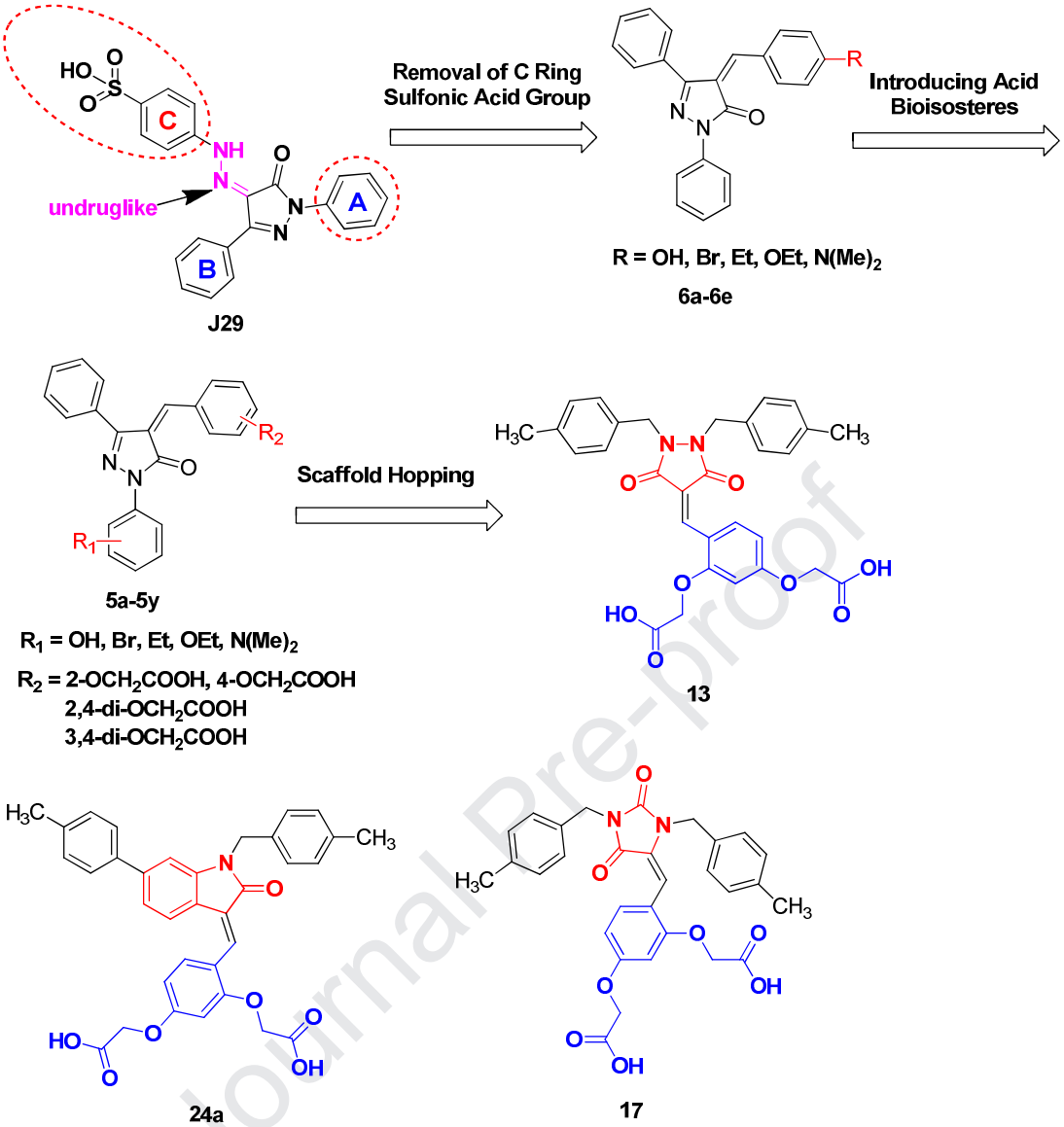

Fig. 3 Hit optimization strategy of the pyrazolone SAP2 inhibitor.

In order to explain the SARs, 2,4-disubstituted derivative **5m** and 3,4-disubstituted derivative **5t** were subjected for molecular docking. As shown in **Fig. 4**, their general binding conformation in the active site of SAP2 was similar to that of inhibitor **J29**. Their C1, C3, C4-rings interacted with the S1', S1 and S2 pockets, respectively. The 2,4- and 3,4-dicarboxylic side chains had different orientations in the S2 pocket. Compound 5m formed four hydrogen bonds with SAP2. The C2 ether oxygen atom and carboxyl group formed two hydrogen bonds with Thr221 and Thr222, respectively. Another two hydrogen bonds were observed between the C4 carboxyl group and Val300 and Asn301. In contrast, compound **5t** only formed three hydrogen bonds with Ile223, Val300 and Asn301. Due to weaker hydrogen bonding

interaction, compound showed decreased SAP2 inhibitory activity.

Table 1. SAP2 inhibitory activity of the pyrazolone inhibitors

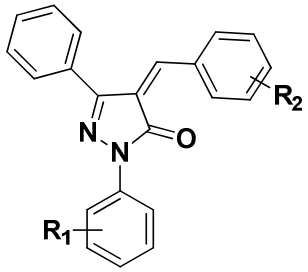

Compd	R_1	R_2	Inhibition (100 μM)	IC_{50} (μM)
5a	H	2-OCH_2COOH	68%	62.15
5b	3-Cl	2-OCH_2COOH	70%	55.48
5c	4-Cl	2-OCH_2COOH	60%	75.15
5d	4-F	2-OCH_2COOH	46%	nd
5e	4-Me	2-OCH_2COOH	63%	72.31
5f	4-OMe	2-OCH_2COOH	64%	70.65
5g	H	4-OCH_2COOH	94%	18.17
5h	3-Cl	4-OCH_2COOH	90%	26.36
5i	4-Cl	4-OCH_2COOH	96%	12.96
5j	4-F	4-OCH_2COOH	71%	39.61
5k	4-Me	4-OCH_2COOH	93%	21.56
5l	4-OMe	4-OCH_2COOH	95%	20.44
5m	H	2,4-diOCH_2COOH	99%	10.05
5n	3-Cl	2,4-diOCH_2COOH	99%	11.54
5o	4-Cl	2,4-diOCH_2COOH	99%	10.75

5p	4-F	2,4-diOCH_2COOH	93%	17.94
5q	4-Me	2,4-diOCH_2COOH	99%	13.53
5r	4-OMe	2,4-diOCH_2COOH	94%	15.67
5s	2,4-diF	2,4-diOCH_2COOH	86%	32.72
5t	H	3,4-diOCH_2COOH	86%	18.46
5u	3-Cl	3,4-diOCH_2COOH	82%	22.72
5v	4-Cl	3,4-diOCH_2COOH	70%	46.86
5w	4-F	3,4-diOCH_2COOH	83%	33.74
5x	4-Me	3,4-diOCH_2COOH	85%	22.34
5y	4-OMe	3,4-diOCH_2COOH	88%	21.47
6a	H	4-OH	12%	nd
6b	H	4-Br	10%	nd
6c	H	4-Et	7%	nd
6d	H	4-OEt	5%	nd
6e	H	4-$N(Me)_2$	11%	nd
PepA	-	-	-	0.028

nd = not determined

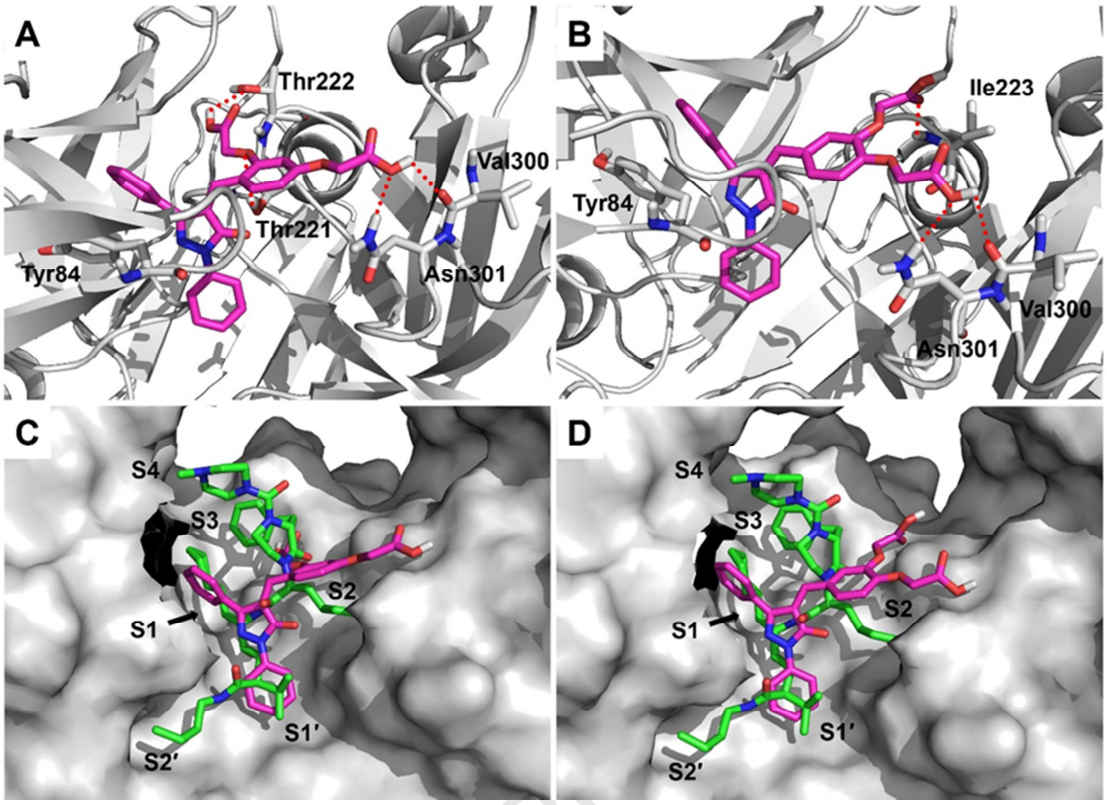

Fig. 4 Binding modes of pyrazolone SAP2 inhibitors **5m** and **5t**. (A, B) Proposed binding pose of inhibitor **5m** and **5t** in the active site of SAP2. The inhibitors are shown in the stick format and hydrogen bonds are shown in dotted red lines. (C, D) The comparison of binding modes of small-molecule inhibitor **5m** and **5t** (carbon atoms in purple) with peptide inhibitor A-70450 (carbon atoms in green) are shown on the surface of SAP2. The ligand binding pockets of SAP2 are labeled on the surface of the active site. The figures are generated using PyMol (http://www.pymol.org).

*2.4 Scaffold Hopping of Pyrazolone SAP2 Inhibitor **5m***

For further investigating the importance of the pyrazolone scaffold and improving the SAP2 inhibition activity, pyrazolidine-3,5-dione (**13**), imidazolidine-2,4-dione (**17**) and indolin-2-one (**24a**) were used to replace pyrazolone. Interestingly, SAP2 inhibitory activates revealed that indolin-2-one derivative **24a** showed the best inhibitory activity (IC_{50} = 0.92 μM, **Table 2**), which was more potent than pyrazolone inhibitor **5m**. Then, the binding mode of inhibitor **24a** and **24c** were investigated by molecule docking (**Fig. 5** and **S2** in Supporting Information). As

shown in **Fig. 5**, the 2,4-dicarboxyl groups formed four hydrogen bonds with Ser36, As24a31, Glu193 and Arg195, respectively. The phenyl group of benzyl side chain formed aromatic π-π interaction with Tyr225. The binding mode of compound **24c** with SAP2 was similar to that of **24a**.

Table 2. SAP2 inhibitory activity of the derivatives of **5m**

Compd	Inhibition（100 μM）	IC_{50}（μM）
13	94%	17.43
17	91%	23.77
24a	100%	0.92
PepA	100%	0.022

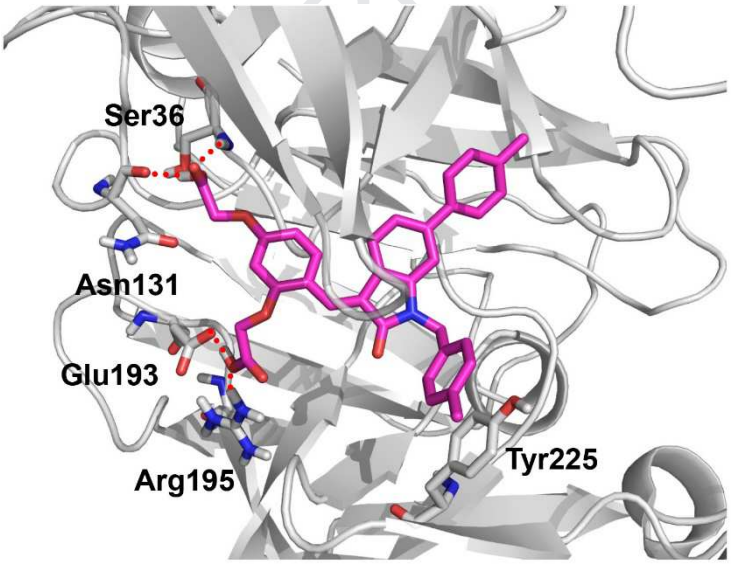

Fig. 5 Binding mode of indolone SAP2 inhibitor **24a**.

2.5 Chemistry

The synthetic routes of the pyrazolone derivatives are outlined in **Schemes 1**. The starting material ethyl 3-oxo-3-phenylpropanoate (**1**) was condensed with various substituted phenylhydrazine hydrochlorides in the presence of AcOH to afford

pyrazolone intermediates **2**. Then, esters 4 were obtained by reacting 2 with various aldehydes containing mono- or di-ester side chain. Finally, after hydrolysis of the ester groups using LiOH, target compounds **5a-5y** were obtained. By a similar route, 1,3-diphenyl-*1H*-pyrazol-5(*4H*)-one (**2**) reacted with various aldehydes in the presence of piperidine and absolute alcohol, and then after hydrolysis of the ester groups to afford target compounds **6a-6e** (**Scheme 2**).

Scheme 1

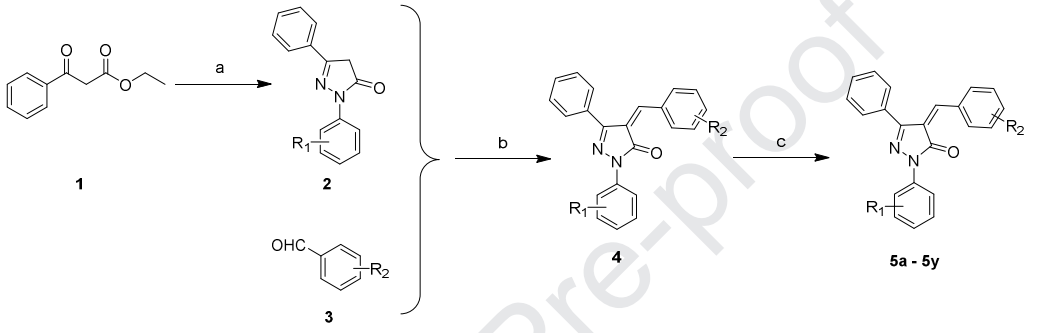

5a R_1 = H, R_2 = 2-OCH_2COOH
5b R_1 = 3-Cl, R_2 = 2-OCH_2COOH
5c R_1 = 4-Cl, R_2 = 2-OCH_2COOH
5d R_1 = 4-F, R_2 = 2-OCH_2COOH
5e R_1 = 4-Me, R_2 = 2-OCH_2COOH
5f R_1 = 4-OMe, R_2 = 2-OCH_2COOH
5g R_1 = H, R_2 = 4-OCH_2COOH
5h R_1 = 3-Cl, R_2 = 4-OCH_2COOH
5i R_1 = 4-Cl, R_2 = 4-OCH_2COOH
5j R_1 = 4-F, R_2 = 4-OCH_2COOH
5k R_1 = 4-Me, R_2 = 4-OCH_2COOH
5l R_1 = 4-OMe, R_2 = 4-OCH_2COOH
5m R_1 = H, R_2 = 2,4-diOCH_2COOH
5n R_1 = 3-Cl, R_2 = 2,4-diOCH_2COOH
5o R_1 = 4-Cl, R_2 = 2,4-diOCH_2COOH
5p R_1 = 4-F, R_2 = 2,4-diOCH_2COOH
5q R_1 = 4-Me, R_2 = 2,4-diOCH_2COOH
5r R_1 = 4-OMe, R_2 = 2,4-diOCH_2COOH
5s R_1 = 2,4-diF, R_2 = 2,4-diOCH_2COOH
5t R_1 = H, R_2 = 3,4-diOCH_2COOH
5u R_1 = 3-Cl, R_2 = 3,4-diOCH_2COOH
5v R_1 = 4-Cl, R_2 = 3,4-diOCH_2COOH
5w R_1 = 4-F, R_2 = 3,4-diOCH_2COOH
5x R_1 = 4-Me, R_2 = 3,4-diOCH_2COOH
5y R_1 = 4-OMe, R_2 = 3,4-diOCH_2COOH

Reagents and conditions: (a) substituted phenylhydrazine hydrochloride, acetic acid, Et_3N, reflux, 3h, 25-57 %; (b) piperidine, absolute alcohol, 60 □, 6 h, 24-85%; (c) LiOH, THF: MeOH: H_2O =3: 2: 1, rt, 6 h, 53-90%.

Scheme 2

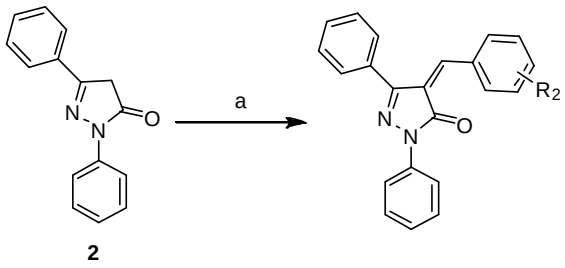

6a R_2 = 4-OH
6b R_2 = 4-Br
6c R_2 = 4-Et
6d R_2 = 4-OEt
6e R_2 = 4-$N(Me)_2$

Reagents and conditions: (a) various aldehyde, piperidine, absolute alcohol, 60℃, 6 h, 65-85 %.

The synthetic route of the pyrazolidinedione derivatives is shown in **Scheme 3**.

Starting from di-tert-butylhydrazine-1,2-dicarboxylate, intermediate **10** was synthesized via electrophilic substitution, deprotection and acylation. By a similar procedure in **Scheme 1**, intermediate **10** reacted with disubstituted benzaldehyde in the presence of piperidine and absolute alcohol to afford target compound **13**. Using a similar protocol, imidazolidine-2,4-dione derivative **17** was synthesized (**Scheme 4**).

Scheme 3

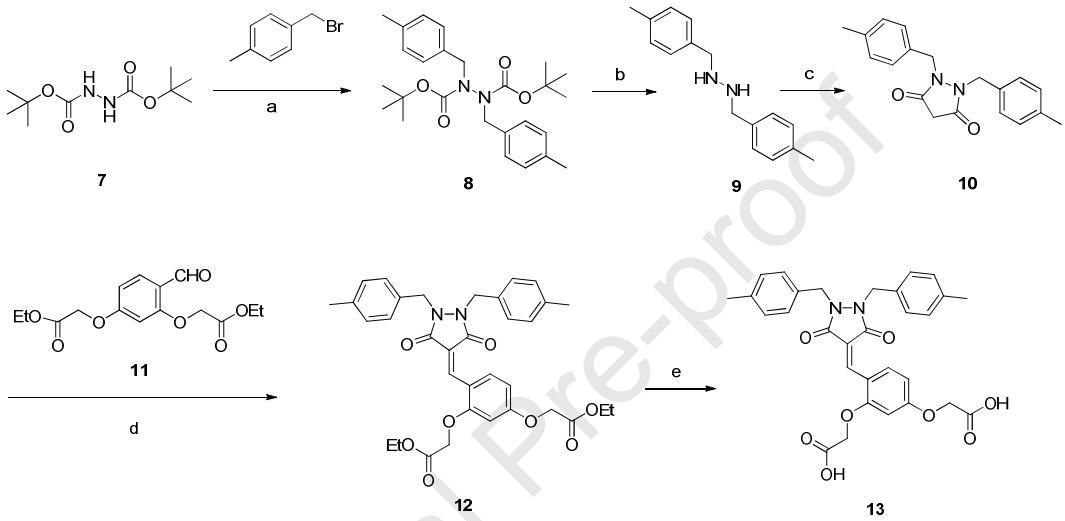

Reagents and conditions: (a) NaH, DMF, 0 □, 4 h; (b) TFA, DCM, rt, 1 h; (c) malonyl dichloride, triethylamine, DCM, 0 □, 0.5 h; (d) piperidine, DCM, rt, overnight; (e) LiOH·H_2O, THF: MeOH: H_2O = 3: 2: 1, rt, 0.5 h.

Scheme 4

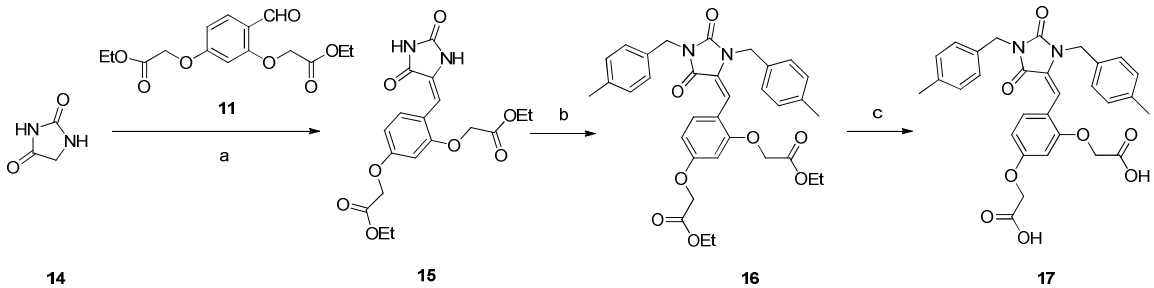

Reagents and conditions: (a) NH_4OAc, AcOH, 115 □, reflux, 6 h; (b) NaH, DMF, 0 □, 4 h; (c) LiOH·H_2O, THF: MeOH: H_2O = 3: 2: 1, rt, 0.5 h.

Indolin-2-one derivatives **24a-24h** were synthesized according to the procedures outlined in **Scheme 5**. Substituted phenylboronic acids were reacted with

6-bromoindolin-2-one to give compound **20**. Following similar synthetic steps, compound **23** reacted with disubstituted benzaldehyde to afford target compounds **24a-24h**.

Scheme 5

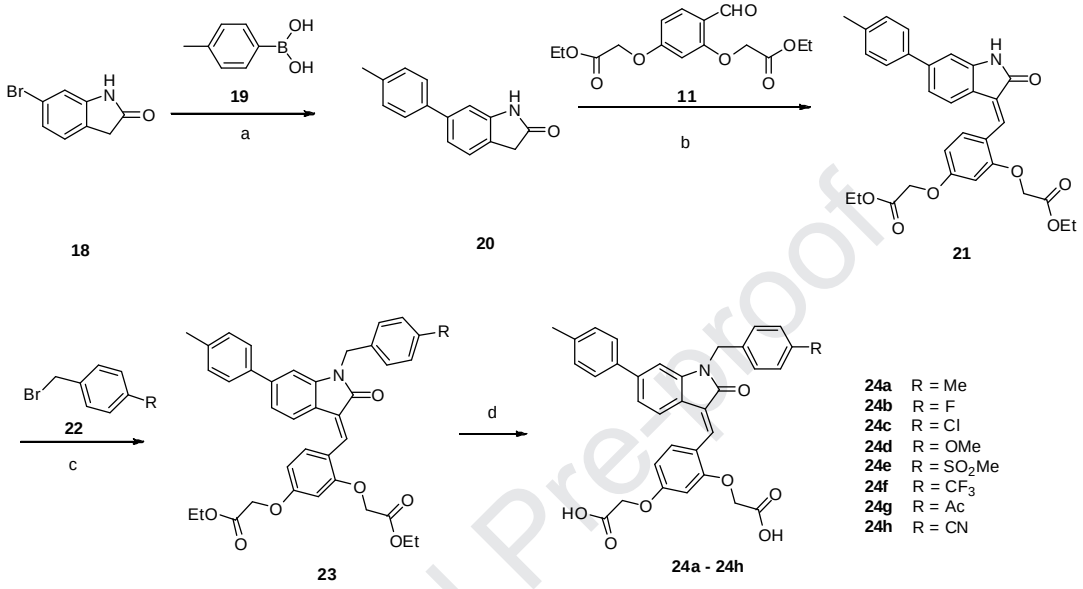

Reagents and conditions: (a) Na_2CO_3, $PdP(ph_3)_4$, PhMe, 100 □, N_2, reflux, 5 h; (b) piperidine, absolute alcohol, 78 □, reflux, 3 h; (c) NaH, DMF, 0□, 4 h; (d) $LiOH \cdot H_2O$, THF: MeOH: H_2O= 3: 2: 1, rt, 1 h.

*2.6 Biological Evaluation and SAR of Inhibitor **24a***

As a promising lead compound for SAP2, a series of novel derivatives of inhibitor **24a** were designed and synthesized (**Scheme 5**). Their SAP2 inhibitory activities are summarized in **Table 3** and **S2** in Supporting Information. Various substituents on benzyl benzene ring were investigated. The SAP2 inhibitory activity was retained for most of the target compounds. Among them, methyl, chloro, methylsulfonyl, trifluoromethyl, and cyano substituents resulted in better activity than fluoride, methoxyl and carboxyl substituents, which inhibited SAP2 100% at concentration of 100 μM. The in vitro antifungal activities of selected target compounds (**24a**, **24c**, **24e**, **24f**) were measured. The results showed that indolone SAP2 inhibitors could not inhibit the growth of *C. albicans* and had no *in vitro*

synergistic effect with FLC (**Tables S3** and **S4** in Supporting Information).

Table 3. SAP2 inhibitory activity of the indolone inhibitors

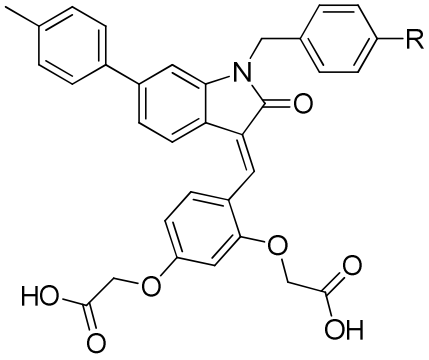

Compd	R	Inhibition (100 μM)
24a	4-Me	100%
24b	4-F	58%
24c	4-Cl	100%
24d	4-OMe	29%
24e	4-SO_2Me	100%
24f	4-CF_3	100%
24g	4-Ac	90%
24h	4-CN	100%
PepA	-	100%

2.7 Compound 24a Inhibited the Formation of Azole-resistant C. albicans and C. tropicalis Biofilms

Due to formation of biofilms, current antifungal treatments are accompanied by therapeutic failure and drug-tolerance [17]. Fungi biofilms are consist of dense layers protecting fungi from antifungal drugs [15, 25, 26]. SAPs are known as virulence factors associated with biofilm and hyphal formation. However, whether SAP2 inhibitors block biofilm and hyphal formation is still unknown. Therefore, selected SAP2 inhibitors were assayed for inhibitory activity against biofilm formation against clinical FLC-resistant *C. albicans* and *C. tropicalis* isolates using FLC as the control

group. The results revealed that compounds **24a**, **24c**, **24e**, **24f** and **24h** dose-dependently inhibited biofilm formation. Among them, inhibitors **24c** and **24h** inhibited *C. albicans* biofilm formation larger than 50% at high concentration (64 μg/mL), while compounds **24a**, **24c** and **24f** achieved more than 50% biofilm formation in *C. tropicalis* cells. In contrast, the inhibition of biofilm formation was lower than 50% when treated with FLC at 64 μg/mL (**Fig. 6A, 6B**). Furthermore, we investigated the synergistic effect compound **24a** in combination with and FLC at different concentrations. The result showed that biofilm formation was effectively inhibited at low concentration (0.5 μg/mL, $P < 0.05$) and nearly 90% inhibition could be achieved at 32 μg/mL (**Fig. 6C**). Thus, SAP2 inhibitor could serve as a potential sensitizer of FLC, providing a new strategy to treat biofilm-related resistant infections.

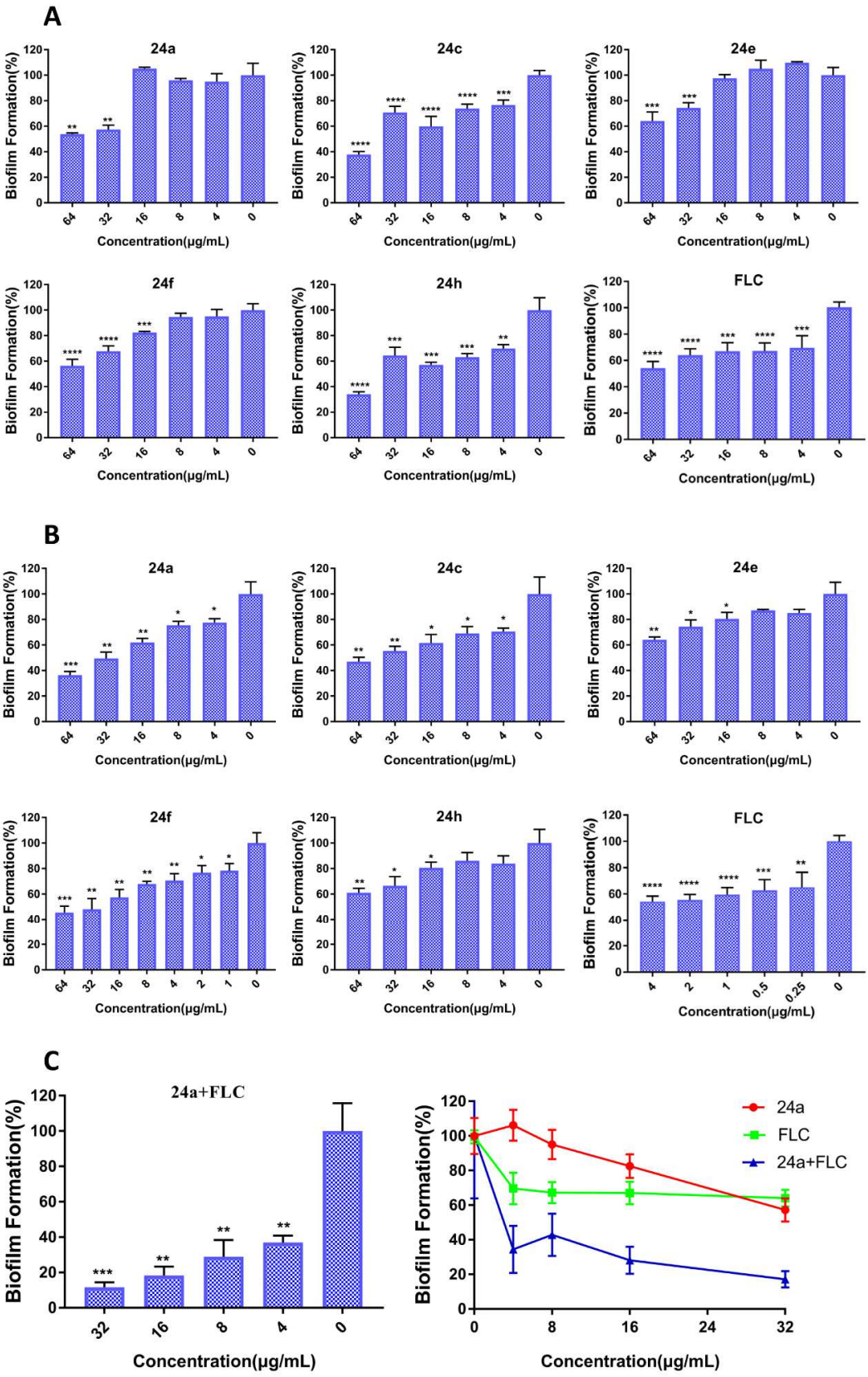

Fig. 6 Inhibition of biofilm formation by SAP2 inhibitors. (A) The biofilm formation of azole-resistant *C. albicans 0304103* on different concentrations of compound **24a**,

24c, **24e**, **24f**, **24h** and FLC. (B) The biofilm formation of azole-resistant *C. tropicalis* 10186 on different concentrations of compound **24a**, **24c**, **24e**, **24f**, **24h** and FLC. (C) The biofilm formation of azole-resistant *C. albicans 0304103* treated with both compound **24a** and FLC. The results were represented as the mean ± SD by three independent experiments. Statistical significance between groups was determined by Student's t test. * $P < 0.05$, ** $P < 0.01$, *** $P < 0.001$, **** $P < 0.0001$.

*2.8 Compound **24a** Inhibited Filamentation of Azole-sensitive and Azole-resistant C. albicans and C. tropicalis*

Hypha contributes to adhesion and invasion into hosts and is essential for biofilm formation [27]. On the basis of the biofilm inhibitory activity, compound **24a** was selected to evaluate the effects on yeast-to-hypha morphological transition of azole-sensitive and azole-resistant *C. albicans* and *C. tropicalis*. As shown in **Fig. 7**, azole-sensitive and azole-resistant *C. albicans* formed long hyphae, while *C. tropicalis* formed short hypha. Compound **24a** inhibited hyphal formation almost completely at high concentration of 128 μg/mL. At lower concentrations (8-32 μg/mL), compound **24a** could not inhibit hyphal formation obviously against both the azole-sensitive and azole-resistant *C. albicans* (**Fig. S3** in Supporting Information). In contrast, compound **24a** showed better hyphae inhibitory activity against azole-resistant *C. tropicalis*. At the concentrations in the range of 4-16 μg/mL, compound **24a** effectively inhibited hyphal formation of azole-resistant *C. tropicalis*. At the high concentration of 64 μg/mL, hyphal formation was completely inhibited (**Fig. 7** and **S3** in Supporting Information). The results suggested that SAP2 inhibitor **24a** had potent inhibition effect against morphological transition of *C. tropicalis*.

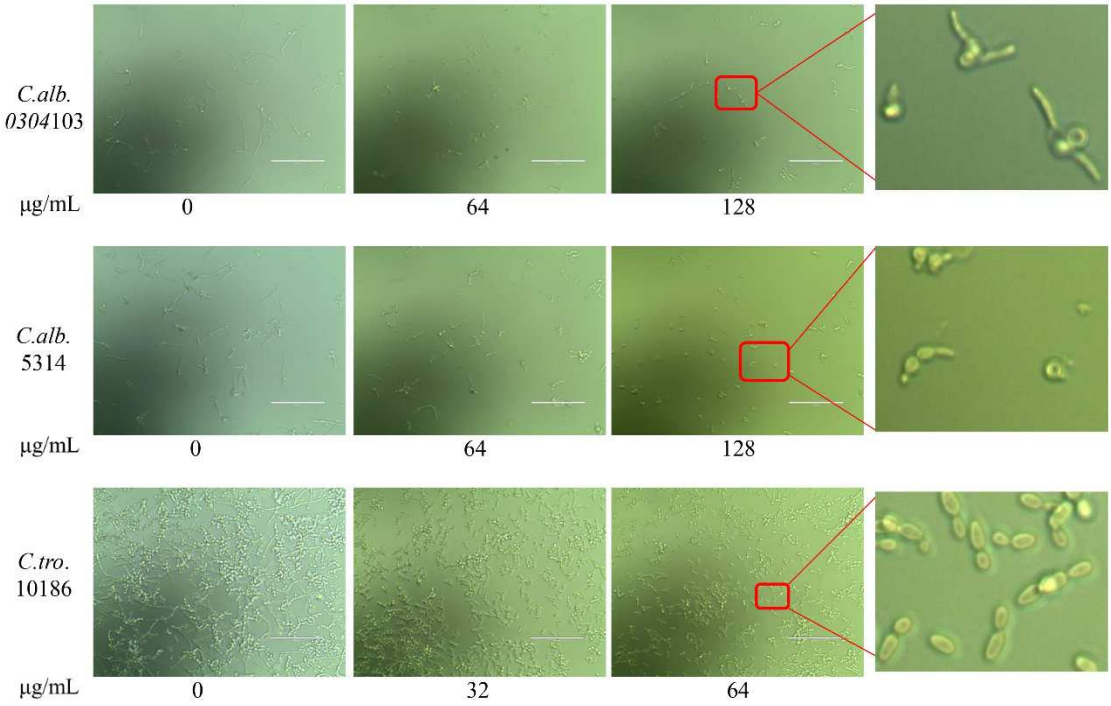

Fig. 7 Inhibition of filamentation by compound **24a**. DIC microscope photographs on filamentation of azole-resistant *C. albicans* 0304103, azole-sensitive *C. albicans* (*C. alb.*) SC5314, azole-resistant *C. tropicalis* (*C. tro.*) 10186.

2.9 Effects of Indolone Compounds on the Expression of SAP2 and Biofilm Formation Related Gene in C. albicans cells

Given the biofilm formation inhibitory effects of compound **24a**, the expression levels of SAP2 and biofilm formation related genes (*ECE1*, *ALS3*, *EFG1*, *TEC1* and *CPH1*) were determined by qRT-PCR. The expression of *SAP2* was down-regulated obviously for compounds **24a, 24c, 24f, 24g** and **24h**, which was consistent well with their SAP2 inhibitory activity (**Fig. 8A**). Extent of cell elongation protein 1 (ECE1) is a cytolytic peptide toxin and damages host epithelial membranes. Agglutinin-like protein 3 (ALS3) acts on the adhesion of yeast-to-host tissue, which is important in biofilm formation. The expressions of *ECE2* and *ALS3* were down-regulated, suggesting that compound **24a** might act on the polarization and adhesion *C.albicans* cells. Enhanced filamentous growth protein 1 (EFG1), transcription activator TEC1

and transcription factor CPH1 are regarded as the critical proteins in signal transduction pathways of hypha growth. EFG1 is involved in cAMP-dependent pathway and is perceived to be a major regulator of hyphae, while CPH1 depends on a MAPK signaling pathway [28]. After the treatment of compound **24a**, *EFG1* was down-regulated and *CPH1* and *TEC1* were up-regulated, indicating that compound **24a** might inhibit hypha growth through the cAMP-dependent pathway. The results could also explain the fact that compound **24a** only inhibited hypha formation on high concentrations (**Fig. 8B**).

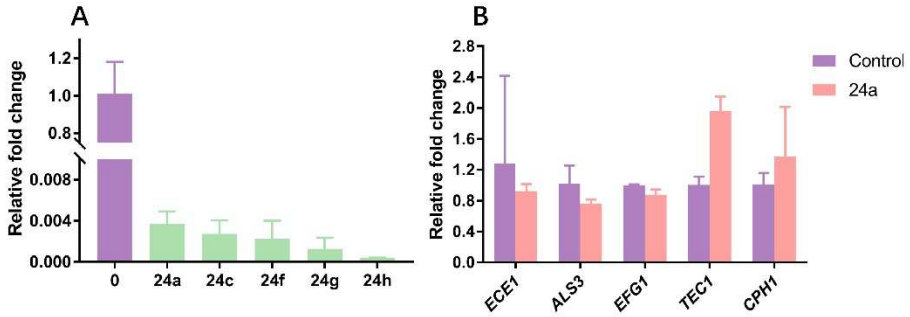

Fig. 8 (A) The effects of compounds **24a, 24c, 24f, 24g** and **24h** on the expression levels of SAP2 gene. (B) The effects of compounds **24a** on the expression of fungal filamentation and biofilm formation related genes. Real-time RT-PCR experiment was used to investigate gene expression changes in *C. albicans* 0304103 strain. The concentration of compounds was 64 μg/mL.

2.10 In vivo Antifungal Activity

To investigate the in vivo antifungal effect of SAP2 inhibitors, an invasive *C. albicans* infectious murine model was constructed by injecting *C. albicans* 0304103 cells into the tail veins. The blank control group was treated with saline, the positive control group was treated with FLC at 10 mg/kg, and the treatment group was administrated with **24a** at 10 mg/kg. Each mouse was injected intraperitoneally once daily and the administration lasted for four days. Then Kidney fungal burdens were determined. The results showed that compound **24a** significantly reduced the fungal burden in the kidney ($P < 0.001$), which was comparable to FLC ($P < 0.0001$, **Fig. 9**).

Thus, SAP2 inhibitor **24a** offered a new lead compound for the potential therapy of invasive candidiasis.

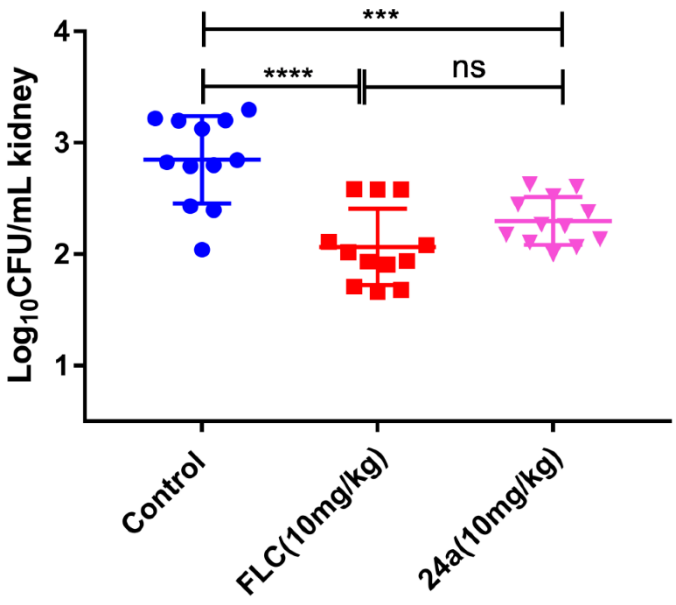

Fig. 9 In vivo activites of compound **24a** and FLC in the *C. albicans* 0304103 infectious murine model. The fungal burden of kidney (in $\log_{10}$ CFU/mL of kidney) were plotted as mean ± SD. Statistical significance between groups was determined by Student's t test. **** $P < 0.0001$, *** $P < 0.001$, ns represents no significant difference.

3. Conclusion

In summary, a series of novel small-molecule SAP2 inhibitors were identified by structure-based virtual screening and rational inhibitor design. After step-by-step lead optimizations, indolinone derivative **24a** was successfully identified with potent SAP2 inhibitory activity. Further biological evaluations indicated that compound **24a** effectively blocked fungi biofilm and hypha formation by down-regulating the expression of genes *SAP2*, *ECE1*, *ALS3* and *EFG1*. In a murine model of invasive candidiasis, compound **24a** showed potent *in vivo* antifungal potency and significantly reduced kidney fungal burdens. Targeting virulence factor is a new strategy for the development of new generation of antifungal agents. The small-molecule SAP2

inhibitors reported herein represent promising antifungal lead compounds. They are also valuable tools to explore the druggability and biological functions of SAP2. Further optimization of SAP2 inhibitors is ongoing.

4. Experimental Section

4.1 Chemistry

The reagents and solvents used in the experiments were commercially available. Column chromatography was performed on 200-400 mesh silica gel. ^{13}C-NMR and ^{1}H-NMR spectra were recorded on Bruker AVANCE600 or AVANCE300 spectrometer (Bruker Company, Germany) with $CDCl_3$ or DMSO-d_6 as the solvents and TMS as the internal. Chemical shift was expressed in ppm (δ). The coupling constant is reported in hertz (Hz). The melting point was measured by a microscope melting point apparatus using an XT4A type temperature control system. The chemical purities were analyzed by high performance liquid chromatography (HPLC) using a flow of 0.4 mL/min on a C18 column with CH_3CN/H_2O as the mobile phase. All target compounds exhibited purities greater than 95%.

*4.1.1. (Z)-2,2'-((4-((5-oxo-1,3-diphenyl-1,5-dihydro-4H-pyrazol-4-ylidene) methyl) -1,3-phenylene)bis(oxy))diacetic acid (**5m**)*

To a solution of intermediate **4** (0.20 g, 0.47 mmol, 1 equiv) in mixed solvent (THF: MeOH: H2O = 3: 2: 1), $LiOH\cdot H_2O$ (0.03 g, 0.71 mmol, 1.5 equiv) was added. The mixture was reacted at room temperature for 0.5 h, then the solvent was removed under reduced pressure. Water (20 mL) and 1M HCl were added to adjust the PH to 2.0 to produce precipitation. Then, the precipitation was filtered, washed with water and recrystallized from ethanol to give compound **5m** (0.14 g, yield: 64%) as a orange solid. m.p.: 230-232 ºC. ^{1}H-NMR (300 MHz, DMSO-d_6) δ: 13.18 (brs, 2H), 9.31 (s, 1H), 8.31 (s, 1H), 7.98 (d, 2H, J = 7.75 Hz), 7.17-7.79 (m, 8H), 6.62-6.81 (m, 2H), 4.86 (s, 2H), 4.83(s, 2H). ^{13}C-NMR (75 MHz, DMSO-*d6*) δ: 169.91, 165.13, 162.50,

161.11, 153.39, 143.82, 138.81, 135.79, 132.74, 131.13, 130.18, 129.44, 129.32, 129.22, 128.84, 128.49, 128.24, 125.36, 121.93, 119.37, 118.83, 116.11, 107.65, 100.27, 66.06, 65.34. ESI-MS (m/z): 473.46 [M+1].

The preparation methods of compounds **5a-5l**, **5n-5y** and **24a-24h** are the same as compound **5m**. Compounds **6a-6e** were prepared in the same way as compound **4**.

*4.1.2. (Z)-3-oxo-3-(4-((5-oxo-1,3-diphenyl-1,5-dihydro-4H-pyrazol-4-ylidene)methyl) phenyl)propanoic acid (**5g**).*

Orange solid, yield: 72%, m.p.: 125-127 ºC. ^{1}H-NMR (300 MHz, DMSO-d_6) δ: 13.25 (br s, 1H), 8.57-8.70 (m, 2H), 7.98 (d, 2H, J = 9.17 Hz), 7.43-7.77 (m, 6H), 7.06-7.41 (m, 5H), 4.83 (s, 2H). 13C-NMR (75 MHz, DMSO-d_6) δ: 191.78, 170.07, 162.91, 162.36, 158.59, 153.39, 150.64, 138.71, 137.47, 132.15, 131.04, 130.26, 129.46, 129.38, 128.81, 128.72, 128.49, 128.29, 126.70, 125.46, 123.03, 119.43, 115.21, 65.31. ESI-MS (m/z): 397.00 [M-1].

*4.1.3. (Z)-3,3'-(4-((1-(3-chlorophenyl)-5-oxo-3-phenyl-1,5-dihydro-4H-pyrazol-4-ylidene)methyl)-1,3-phenylene)bis(3-oxopropanoic acid) (**5n**)*

Orange solid, yield: 73%, m.p.: 228-229 ºC. ^{1}H-NMR (300 MHz, DMSO-d_6) δ: 13.20 (br s, 2H), 9.27 (s, 1H), 8.33 (s, 1H), 7.89-8.17 (m, 2H), 7.43-7.80 (m, 6H), 7.29 (d, 1H, J = 7.99 Hz), 6.63-6.86 (m, 2H), 4.86 (s, 2H), 4.82 (s, 2H). ^{13}C-NMR (75 MHz, DMSO-d_6) δ: 169.88, 165.35, 162.68, 161.26, 153.96, 144.37, 140.02, 135.86, 133.76, 131.13, 130.91, 130.32, 129.46, 129.27, 128.89, 128.28, 127.92, 124.87, 121.51, 118.39, 117.30, 116.07, 107.77, 100.26, 66.07, 65.36. ESI-MS (m/z): 505.11 [M-1].

*4.1.4. (Z)-3,3'-(4-((1-(4-chlorophenyl)-5-oxo-3-phenyl-1,5-dihydro-4H-pyrazol-4-ylidene) methyl)-1,3-phenylene) bis (3-oxopropanoic acid) (**5o**).*

Orange solid, yield: 76%, m.p.: 241-243 ºC. ^{1}H-NMR (300 MHz, DMSO-d_6) δ: 13.17 (brs, 2H), 9.29 (s, 1H), 8.32 (s, 1H), 8.03 (d, 2H, J = 9.00 Hz), 7.41-7.82 (m, 7H), 6.63-6.80 (m, 2H), 4.86 (s, 2H), 4.82 (s, 2H). ^{13}C-NMR (75 MHz, DMSO-d_6) δ: 169.89, 165.28, 162.52, 161.22, 153.75, 144.19, 137.64, 135.81, 130.98, 130.65,

130.27, 129.45, 129.28, 129.24, 129.07, 128.85, 128.27, 127.19, 121.62, 120.66, 116.08, 107.74, 100.26, 66.08, 65.36. ESI-MS (m/z): 505.00 [M-1].

*4.1.5. (Z)-3,3'-(4-((5-oxo-1,3-diphenyl-1,5-dihydro-4H-pyrazol-4-ylidene) methyl) -1,2-phenylene) bis (3-oxopropanoic acid) (**5t**).*

Orange solid, yield:85%, m.p.: 252-253 ºC. ^{1}H-NMR (300 MHz, DMSO-d_6) δ: 13.11 (brs, 2H), 8.65 (s, 1H), 7.91-8.14 (m, 3H), 7.40-7.80 (m, 8H), 7.00-7.29 (m, 2H), 4.89 (s, 2H), 4.79 (s, 2H). ^{13}C-NMR (75 MHz, DMSO-d_6) δ: 170.19, 170.01, 162.41, 153.41, 152.79, 150.87, 147.06, 138.70, 131.26, 131.04, 130.25, 129.45, 129.41, 129.37, 129.06, 128.54, 126.88, 125.50, 123.18, 119.53 (2C), 118.95, 118.48, 113.25, 65.38, 65.34. ESI-MS (m/z): 573.31 [M+1].

*4.1.6. (Z)-4-(4-hydroxybenzylidene)-2,5-diphenyl-2,4-dihydro-3H-pyrazol-3-one (**6a**).*

Orange solid, yield: 65%, m.p.: 242-243 ºC. ^{1}H-NMR (300 MHz, DMSO-d_6) δ: 10.94 (s, 1), 8.53-8.69 (m, 2), 8.00 (d, 2H, J = 7.92 Hz), 7.39-7.80 (m, 8H), 7.16-7.32 (m, 1H), 6.94 (d, 2H, J = 8.16 Hz). ^{13}C-NMR (75 MHz, DMSO-d_6) δ: 191.40, 163.94, 163.77, 162.50, 153.48, 151.08, 138.83, 138.28, 132.55, 131.21, 130.16, 129.42, 129.38, 129.32, 129.02, 128.90, 128.52, 125.33, 125.18, 121.66, 119.36, 116.30. ESI-MS (m/z): 341.45 [M+1].

*4.1.7. (E)-2,2'-((4-((1-(4-methylbenzyl)-2-oxo-6-(p-tolyl) indolin-3-ylidene) methyl)-1,3-phenylene) bis (oxy)) diacetic acid (**24a**).*

Orange solid, yield: 79.5%. ^{1}H-NMR (600 MHz, DMSO-d_6) δ: 13.11 (s, 2H), 7.84 (s, 1H), 7.75 (d, J = 8.1 Hz, 1H), 7.65 (d, J = 7.8 Hz, 1H), 7.51 (d, J = 7.4 Hz, 2H), 7.24 (t, J = 7.7 Hz, 4H), 7.21 (s, 1H), 7.19 (d, J = 7.3 Hz, 1H), 7.12 (d, J = 7.5 Hz, 2H), 6.67 (d, J = 8.4 Hz, 2H), 5.02 (s, 2H), 4.86 (s, 2H), 4.77 (s, 2H), 2.31 (s, 3H), 2.22 (s, 3H). ESI-MS (m/s): 564.40 [M+1], 562.28 [M-1]. ^{13}C-NMR (150 MHz, DMSO-d_6) δ: 129.49, 129.17, 127.26, 126.38, 42.32, 40.04, 39.84, 39.63 (d, J = 21.0 Hz), 39.42, 39.31, 39.21, 20.61. HRMS m/z calcd for $C_{34}H_{25}N_2O_7$ [M-H]- 562.1871, found 562.18923. HPLC purity 95.62 %. Retention time: 5.649 min, eluted with

CH_3CN: H_2O = 4: 1.

*4.1.8. (E)-2,2'-((4-((1-(4-chlorobenzyl)-2-oxo-6-(p-tolyl) indolin-3-ylidene) methyl) -1,3-phenylene) bis(oxy)) diacetic acid (**24c**).*

Orange solid, yield: 62.7%. ^{1}H-NMR (600 MHz, DMSO-d_6) δ: 13.01 (s, 2H), 7.88 (s, 1H), 7.79 (d, *J* = 8.3 Hz, 1H), 7.70 (d, *J* = 8.1 Hz, 1H), 7.55 (d, *J* = 8.2 Hz, 2H), 7.41 (d, *J* = 8.4 Hz, 4H), 7.30-7.25 (m, 3H), 7.25-7.22 (m, 1H), 6.71 (d, *J* = 9.7 Hz, 2H), 5.10 (s, 2H), 4.88 (s, 2H), 4.80 (s, 2H), 2.34 (s, 3H). ^{13}C-NMR (150 MHz, DMSO-d_6) δ: 169.75, 169.71, 161.12, 158.10, 143.14, 141.23, 137.29, 136.71, 135.88, 132.53, 131.92, 130.80, 129.48, 129.16, 128.62, 126.42, 123.86, 122.35, 119.89, 119.72, 116.18, 107.04, 106.42, 100.24, 64.99, 64.65, 41.92, 20.64.

*4.1.9. (E)-2,2'-((4-((2-oxo-6-(p-tolyl)-1-(4-(trifluoromethyl) benzyl) indolin-3-ylidene) methyl)-1,3-phenylene) bis(oxy)) diacetic acid (**24f**).*

Orange solid, yield: 95.7%. ^{1}H NMR (600 MHz, DMSO-*d6*) δ 13.05 (s, 2H), 7.87 (s, 1H), 7.79 (d, *J* = 8.4 Hz, 1H), 7.71 (m, *J* = 13.4, 8.2 Hz, 3H), 7.59 (d, *J* = 8.0 Hz, 2H), 7.54 (d, *J* = 8.2 Hz, 2H), 7.29 (s, 1H), 7.27 – 7.23 (m, 3H), 6.72 – 6.68 (m, 2H), 5.20 (s, 2H), 4.88 (s, 2H), 4.79 (s, 2H), 2.33 (s, 3H). ^{13}C-NMR (150 MHz, DMSO-d_6) δ: 169.73, 169.69, 167.98, 161.13, 158.10, 143.13, 141.72, 141.29, 137.31, 136.67, 132.60, 130.81, 129.47, 127.94, 126.43, 125.55, 123.81, 122.39, 119.97, 119.73, 116.18, 106.98, 106.45, 100.25, 65.10, 64.82, 42.23, 20.63.

*4.1.10. (E)-2,2'-((4-((1-(4-acetylbenzyl)-2-oxo-6-(p-tolyl) indolin-3-ylidene) methyl) -1,3-phenylene) bis(oxy))diacetic acid (**24g**).*

Orange solid, yield: 63.6%. ^{1}H-NMR (600 MHz, DMSO-d_6) δ :13.02 (s, 2H), 7.93 (d, *J* = 8.3 Hz, 2H), 7.88 (s, 1H), 7.79 (d, *J* = 8.4 Hz, 1H), 7.69 (d, *J* = 8.0 Hz, 1H), 7.53 (d, *J* = 8.1 Hz, 2H), 7.49 (d, *J* = 7.4 Hz, 2H), 7.27-7.22 (m, 4H), 6.69 (s, 1H), 6.64 (s, 1H), 5.17 (d, *J* = 10.2 Hz, 2H), 4.87 (s, 2H), 4.79 (s, 2H), 2.53 (d, *J* = 6.0 Hz, 3H), 2.32 (d, *J* = 4.8 Hz, 3H). ^{13}C-NMR (150 MHz, DMSO-d_6) δ :197.37, 169.76, 169.72, 167.95, 161.13, 158.11, 143.17, 142.16, 141.23, 137.29, 136.70, 135.98, 132.58, 130.81, 129.47, 128.63, 127.35, 126.41, 123.84, 122.36, 119.91, 119.82,

116.18, 107.07, 106.44, 100.24, 65.13, 64.84, 42.39, 26.61, 20.62.

*4.1.11. (E)-2,2'-((4-((1-(4-cyanobenzyl)-2-oxo-6-(p-tolyl) indolin-3-ylidene) methyl) -1,3-phenylene)bis(oxy))diacetic acid (**24h**).*

Orange solid, yield: 76.5%. ^{1}H NMR (600 MHz, DMSO-*d6*) δ 13.19 (s, 2H), 7.87 (s, 1H), 7.84 – 7.77 (m, 3H), 7.70 (d, *J* = 8.0 Hz, 1H), 7.58 – 7.51 (m, 4H), 7.29 – 7.22 (m, 4H), 6.70 (d, *J* = 10.4 Hz, 2H), 5.19 (s, 2H), 4.87 (s, 2H), 4.79 (s, 2H), 2.32 (s, 3H). ^{13}C-NMR (150 MHz, DMSO-d_6) δ: 170.28, 170.25, 168.48, 161.64, 158.60, 143.52, 143.14, 141.77, 137.82, 137.11, 133.10, 131.32, 129.96, 128.54, 126.92, 124.19, 122.89, 120.50, 120.20, 119.15, 116.61, 110.62, 107.44, 106.88, 100.69, 65.90, 65.43, 60.21, 42.82, 21.12. HRMS m/z calcd for $C_{34}H_{25}N_2O_7$ [M-H]- 573.1667, found 573.16796.

4.2 *Biological activity*

4.2.1 Strains, Culture and Reagents

Strains were routinely incubated in YPD (1% yeast extract, 2% peptone and 2% dextrose) at 30°C in a shaking incubator. *C. albicans* SC5314, *C. albicans* 0304103, *C. tropicalis* 10186 strains were provided by Changzheng Hospital of Shanghai, China. Stock solutions of all compounds were prepared in DMSO at 2 mg/mL.

4.2.2 Biofilm Formation Assay

Suspension of *C. alb.*0304103 (1.0 × 105 CFU/mL) or *C. tro* 10186 cells (1.0 × 105 CFU/mL) was added to a 96-well plate and incubated at 37□ for 90 minutes. Then rinse with PBS medium three times. Subquently, compounds were added at different concentrations with FLC as the positive control. Then the fungi were cultured at 37□ for 24h. Finally, a semi-quantitative determination of biofilm formation was performed using XTT reduction method.

4.2.3 Hyphal Formation Assay

C. alb. 0304103, *C.alb.*SC5314 and *C. tro.*10186 cells suspension (1.0 × 105

CFU/mL in 1.5 mL) were added to a 12-well plate (Corning, USA) and treated by different concentrations of compound 24a with FLC as the positive drug. Then, microscopic observation and photographing were conducted to observe and record the growth of hyphae in each group after incubation at 37 ° C for 3h (*C.alb*. 0304103, *C.alb*.5314) or 7 h (*C. tro*. 10186).

4.2.4 In vivo Antifungal Potency

Female ICR mice (20 ~ 25 g in weight) were used as experimental animals. The immunodeficient mouse model was established by intraperitoneal injection with 0.2 mL cyclophosphamide (100 mg/kg, saline). After 24 hours, 0.2 mL (1 × 105 CFU/mL) of *C. albicans* 0304103 was injected by intravenous. Mice were divided into three groups with 4 mice in each group. FLC (10 mg/kg) and compound 24a (10 mg/kg) were injected intraperitoneally 24 h after inoculation. After four consecutive days of administration, mice were sacrificed. Kidney tissue was removed and homogenized. The total fungal load was calculated by spreading a certain dilution on the YPD agar, and incubatione at 30 ° C.

4.2.5 SAP2 Inhibitory Activity Assay.

To asses the SAP2 inhibitory activity, FRET assay was performed. SAP2 enzyme was expressed and purified by Wuxi Biortus Biosciences Co. Ltd. (Wuxi, China). The FRET pair-labeled substrate (Dabcyl-Arg-Lys-Pro-Ala-Leu-Phe-Phe-Arg-Leu-Glu (EDANS)-Arg-OH) was synthesized and purchased from GL Biochem (Shanghai) Ltd. A 50 mM sodium citrate buffer (pH = 4.5) containing 50 mM NaCl was prepared as assay buffer. The reaction mixture contained 185 µL buffer and 5 µL SAP2 solution (a linear fluorescence increase of 100 units/min). The text compounds were diluted in DMSO, and 5 µL of the dilution was added and preincubated with SAP2 for 30 min before the addition of substrate. The final concentrations of text compounds were between 100 µM and 0.01 µM (10 µM ~ 0.001 nM for pepstatin A). Finally, 5 µL substrate solution (18.75 µM in DMSO) was added and the mixture was incubated at 30 °C for 30 min in a final volume of 200 µL. Fluorescence was determined by

Bioteck Synergy2 spectrophotometer using a microplate reader (λ_{ex} = 340/30 nm, λ_{em} = 485/20 nm). The curve fitting was performed by nonlinear regression with normalized dose−response fit and IC_{50} values were calculated using GraphPad Prism software.

Acknowledgments

This work was supported by the National Natural Science Foundation of China (Grants 81725020 and 81573283 to C. S., 81973175 to N.L.), Natural Science Foundation of Shanghai (18ZR1449200 to S.W.), the Innovation Program of Shanghai Municipal Education Commission (Grant 2019-01-07-00-07-E00073 to C.S.) and Science and Technology Commission of Shanghai Municipality (Grant 17XD1404700).

Appendix A. Supplementary data

Supplementarymaterial related to this article can be found in the online version, at doi:

References

[1] G. Brown, D. Denning, N. Gow, S. Levitz, M. Netea, T. White, Hidden killers: human fungal infections. Sci Transl Med 4: 165rv13, in, 2012.

[2] M.C. Fisher, N.J. Hawkins, D. Sanglard, S.J. Gurr, Worldwide emergence of resistance to antifungal drugs challenges human health and food security, Science, 360 (2018) 739-742.

[3] D. Farmakiotis, D.P. Kontoyiannis, Epidemiology of antifungal resistance in human pathogenic yeasts: current viewpoint and practical recommendations for management, International journal of antimicrobial agents, 50 (2017) 318-324.

[4] P. Van Dijck, J. Sjollema, B.P. Cammue, K. Lagrou, J. Berman, C. d'Enfert, D.R. Andes, M.C. Arendrup, A.A. Brakhage, R. Calderone, Methodologies for in vitro and in vivo evaluation of efficacy of antifungal and antibiofilm agents and surface coatings against fungal biofilms, Microbial Cell, 5 (2018) 300.

[5] M. Schaller, C. Borelli, H.C. Korting, B. Hube, Hydrolytic enzymes as virulence factors of Candida

albicans, Mycoses, 48 (2005) 365-377.

[6] M.A. Ghannoum, Potential Role of Phospholipases in Virulence and Fungal Pathogenesis, Clinical Microbiology Reviews, 13 (2000) 122-143.

[7] M. Rapala□Kozik, O. Bochenska, D. Zajac, J. Karkowska□Kuleta, M. Gogol, M. Zawrotniak, A. Kozik, Extracellular proteinases of Candida species pathogenic yeasts, Molecular oral microbiology, 33 (2018) 113-124.

[8] J. Dostál, M. Merkerová, Z. Vinterová, I. Pichová, O. Hrušková-Heidingsfeldová, Two SAPP2 gene homologs are present in Candida parapsilosis genome, Folia microbiologica, 60 (2015) 373-374.

[9] P. Horváth, J.D. Nosanchuk, Z. Hamari, C. Vágvölgyi, A. Gácser, The identification of gene duplication and the role of secreted aspartyl proteinase 1 in Candida parapsilosis virulence, Journal of infectious diseases, 205 (2012) 923-933.

[10] C. Zaugg, M. Borg-von Zepelin, U. Reichard, D. Sanglard, M. Monod, Secreted Aspartic Proteinase Family ofCandida tropicalis, Infection and immunity, 69 (2001) 405-412.

[11] B. Parra-Ortega, H. Cruz-Torres, L. Villa-Tanaca, C. Hernández-Rodríguez, Phylogeny and evolution of the aspartyl protease family from clinically relevant Candida species, Memórias do Instituto Oswaldo Cruz, 104 (2009) 505-512.

[12] W. Aoki, N. Kitahara, N. Miura, H. Morisaka, Y. Yamamoto, K. Kuroda, M. Ueda, Comprehensive characterization of secreted aspartic proteases encoded by a virulence gene family in Candida albicans, The Journal of Biochemistry, 150 (2011) 431-438.

[13] A. Belmadani, A. Semlali, M. Rouabhia, Dermaseptin□S1 decreases Candida albicans growth, biofilm formation and the expression of hyphal wall protein 1 and aspartic protease genes, Journal of applied microbiology, 125 (2018) 72-83.

[14] J. Tu, Z. Li, Y. Jiang, C. Ji, G. Han, Y. Wang, N. Liu, C. Sheng, Discovery of carboline derivatives as potent antifungal agents for the treatment of Cryptococcal meningitis, Journal of medicinal chemistry, 62 (2019) 2376-2389.

[15] N. Liu, H. Zhong, J. Tu, Z. Jiang, Y. Jiang, Y. Jiang, Y. Jiang, J. Li, W. Zhang, Y. Wang, Discovery of simplified sampangine derivatives as novel fungal biofilm inhibitors, European journal of medicinal chemistry, 143 (2018) 1510-1523.

[16] N. Liu, J. Tu, G. Dong, Y. Wang, C. Sheng, Emerging New Targets for the Treatment of Resistant Fungal Infections, J Med Chem, 61 (2018) 5484-5511.

[17] S. Wu, Y. Wang, N. Liu, G. Dong, C. Sheng, Tackling fungal resistance by biofilm inhibitors, Journal of medicinal chemistry, 60 (2017) 2193-2211.

[18] A.U. Mores, R.D. Souza, L. Cavalca, A. de Paula e Carvalho, L.C. Gursky, R.T. Rosa, L.P. Samaranayake, E.A.R. Rosa, Enhancement of Secretory Aspartyl Protease production in biofilms of Candida albicans exposed to sub□inhibitory concentrations of fluconazole, Mycoses, 54 (2011) 195-201.

[19] G. Dong, Y. Liu, Y. Wu, J. Tu, S. Chen, N. Liu, C. Sheng, Novel non-peptidic small molecule inhibitors of secreted aspartic protease 2 (SAP2) for the treatment of resistant fungal infections, Chemical Communications, 54 (2018) 13535-13538.

[20] C. Büchold, Y. Hemberger, C. Heindl, A. Welker, B. Degel, T. Pfeuffer, P. Staib, S. Schneider, P.J. Rosenthal, J. Gut, New cis□Configured Aziridine□2□carboxylates as Aspartic Acid Protease Inhibitors, ChemMedChem, 6 (2011) 141-152.

[21] B. Degel, P. Staib, S. Rohrer, J. Scheiber, E. Martina, C. Büchold, K. Baumann, J. Morschhäuser, T. Schirmeister, Cis□Configured Aziridines Are New Pseudo□Irreversible Dual□Mode Inhibitors of Candida albicans Secreted Aspartic Protease 2, ChemMedChem: Chemistry Enabling Drug Discovery, 3 (2008) 302-315.

[22] Y. Liu, W. Kati, C.-M. Chen, R. Tripathi, A. Molla, W. Kohlbrenner, Use of a fluorescence plate reader for measuring kinetic parameters with inner filter effect correction, Analytical biochemistry, 267 (1999) 331-335.

[23] J.O. Capobianco, C.G. Lerner, R.C. Goldman, Application of a fluorogenic substrate in the assay of proteolytic activity and in the discovery of a potent inhibitor of Candida albicans aspartic proteinase, Analytical biochemistry, 204 (1992) 96-102.

[24] Birchmeier, Walter; Rademann, Joerg; Grosskopf, Stefanie.WO. pantent 128909, Dec 7, 2006.

[25] R.M. Donlan, J.W. Costerton, Biofilms: survival mechanisms of clinically relevant microorganisms, Clinical Microbiology Reviews, 15 (2002) 167-193.

[26] D.D. Li, L.X. Zhao, E. Mylonakis, G.H. Hu, Y. Zou, T.K. Huang, L. Yan, Y. Wang, Y.Y. Jiang, In vitro and in vivo activities of pterostilbene against Candida albicans biofilms, Antimicrob Agents Chemother, 58 (2014) 2344-2355.

[27] Z. Jiang, N. Liu, D. Hu, G. Dong, Z. Miao, J. Yao, H. He, Y. Jiang, W. Zhang, Y. Wang, C. Sheng, The discovery of novel antifungal scaffolds by structural simplification of the natural product

sampangine, Chem Commun (Camb), 51 (2015) 14648-14651.

[28] P.E. Sudbery, Growth of Candida albicans hyphae, Nature Reviews Microbiology, 9 (2011) 737-748.

Research Highlights

- A series of novel SAP2 inhibitors were successfully identified by virtual screening and hit optimization.
- Indolone inhibitor **24a** showed potent SAP2 inhibitory activity and blocked fungi biofilm and hypha formation.
- Compound **24a** showed potent in vivo efficacy in a murine model of invasive candidiasis.

Declaration of interests

☒ The authors declare that they have no known competing financial interests or personal relationships that could have appeared to influence the work reported in this paper.

☐The authors declare the following financial interests/personal relationships which may be considered as potential competing interests: